Applied Geochemistry 189 (2025) 106458

Contents lists available at ScienceDirect

Applied Geochemistry

journal homepage: www.elsevier.com/locate/apgeochem

Comparing open versus closed system weathering experiments using lithium isotopes

Philip A.E. Pogge von Strandmann [a,b,*], Xiaoqing He [a,c], Ying Zhou [a], David J. Wilson [b]

[a] Mainz Geochemistry and Isotope Centre (MIGHTY), Johannes Gutenberg University, Mainz, Germany
[b] London Geochemistry and Isotope Centre (LOGIC), University College London, London, UK
[c] School of Carbon Neutrality Science and Engineering, Anhui University of Science and Technology, Hefei, 231131, China

ARTICLE INFO

Editorial handling by Dr Jiubin Chen

Keywords:
Weathering
Li isotope fractionation
Experiments
Enhanced weathering

ABSTRACT

Chemical weathering of silicate rocks represents a critical part of the carbon cycle, and also a potential method for the artificial drawdown of atmospheric CO_2 ("enhanced weathering"). However, weathering and particularly the resulting secondary minerals (especially clays) have proven hard to measure and quantify. Here we use lithium isotopes to examine and compare two different types of laboratory weathering experiments, using the same initial water and rock, in order to determine their similarities and differences. Specifically, we compare "open system" experiments, where the reacting water drips through the rock powder, with "closed system" experiments, where the reacting water and rock are in contact in a closed beaker. The results (elemental ratios, mobility calculations, saturation indices) suggest that closed experiments, with their longer water-rock interactions times, exhibit more secondary minerals formation. This finding is confirmed by their higher "equilibrium" solution δ^7Li values (δ^7Li = 35.7 versus 29.5 ‰, respectively). The determination of their observed fractionation factors ($\alpha = 0.983 \pm 0.004$ and 0.977 ± 0.003 for the open and closed experiments, respectively) and partition coefficients between water and secondary minerals yields a test case, to determine whether the amount of clays that form during weathering can be calculated solely from Li isotope ratios, giving values similar to the amount of basalt dissolved. Based on potassium concentration (here the most mobile element), 1.9–3.2 g of rock was dissolved. Based on the Li isotopes, 1.6–2.0 g of clay was precipitated during the month-long experiment. This result agrees with other estimates from isotope systems, which suggest that clay formation is rapid, which in turn has consequences for weathering processes, and especially for the efficiency of enhanced weathering.

1. Introduction

The chemical weathering of silicate rocks is considered to be one of the primary methods for sequestering atmospheric CO_2, and hence controlling climate (e.g. Walker et al., 1981; West et al., 2005). During dissolution of silicates in carbonic acid (i.e. dissolved CO_2), cations are released, which are then transported through rivers to the oceans. Here, some cations (mainly Ca and Mg, but also some other elements like Fe) and the dissolved carbon form carbonates, which sequester CO_2 for geological timescales (Berner, 2003). At the same time, other cations and anions released during weathering (e.g. P, K, Fe, Zn) fertilise primary productivity in rivers and the coastal oceans, which takes up CO_2 into organic carbon (France-Lanord and Derry, 1997). In addition, clays and oxides form as a by-product of chemical weathering. They not only enhance organic carbon growth, because microbes leach nutrients from them (Grimm et al., 2019), but they also help to bury that organic carbon in sediments (Kennedy et al., 2014; Kennedy and Wagner, 2011; Lalonde et al., 2012), further sequestering CO_2 for geological timescales. Chemical weathering thus drives CO_2 drawdown on a variety of scales and timescales.

The artificial acceleration of weathering ("enhanced rock weathering", ERW) is also being studied as a potential negative emissions technology (Hartmann et al., 2013). During ERW, fine-grained silicates, such as basalt, would be added to agricultural fields to increase the natural weathering rate, with the aim of accelerating carbon removal from the atmosphere.

This interest has led to a large body of literature examining both modern and past chemical weathering processes, and also a continuing

* Corresponding author. Mainz Geochemistry and Isotope Centre (MIGHTY), Johannes Gutenberg University, Mainz, Germany.
E-mail address: ppoggevo@uni-mainz.de (P.A.E. Pogge von Strandmann).

https://doi.org/10.1016/j.apgeochem.2025.106458
Received 2 July 2024; Received in revised form 6 April 2025; Accepted 26 May 2025
Available online 26 May 2025

search for proxies for various aspects of weathering and its associated carbon sequestration. The stable isotopes of lithium (^{6}Li and ^{7}Li) have increasingly been shown to have high potential for use in this field (e.g. Pogge von Strandmann et al., 2020). A key strength is that Li is present in silicates in concentrations orders of magnitude greater than in carbonates, and hence its behaviour is entirely dominated by silicate weathering (Kisakürek et al., 2005), which is the process of interest in CO_2 sequestration. The Li isotope ratio (δ^7Li) has a fairly narrow range in primary silicate rocks (δ^7Li of the mean continental crust = 0.6 ± 0.6 ‰ (Sauzéat et al., 2015), and 3–5‰ in basalts (Elliott et al., 2006)), and this δ^7Li value is transferred to surface waters during congruent rock dissolution. However, during secondary mineral (clays, oxides, zeolites) formation during weathering, known as incongruent weathering, ^{6}Li is preferentially taken up (adsorbed and incorporated) by the solid phases (Hindshaw et al., 2019; Pistiner and Henderson, 2003), leaving the residual waters isotopically heavy (δ^7Li of river waters = 2–43 ‰) (Dellinger et al., 2015; Huh et al., 1998; Murphy et al., 2019; Pogge von Strandmann et al., 2017). The corresponding secondary phases tend to be isotopically light, but they also tend to become isotopically heavier as this process progresses since they form from increasingly heavy waters with an approximately constant isotopic fractionation factor (Pogge von Strandmann et al., 2023). Lithium isotopes in surface waters are also not noticeably altered by Li uptake into plants (Clergue et al., 2015; Lemarchand et al., 2010), or by primary productivity (Pogge von Strandmann et al., 2016).

Lithium isotope ratios in surface waters are therefore set by the ratio of primary silicate mineral dissolution to secondary mineral formation, making them a useful tracer for the silicate weathering intensity, i.e. the ratio of the weathering rate to the denudation rate (Bouchez et al., 2013; Dellinger et al., 2015). This property has been used in numerous studies of modern rivers (e.g. Dellinger et al., 2015; Pogge von Strandmann et al., 2023), as well as in interpreting archives of palaeo-river waters or seawater (e.g. Krause et al., 2023; Misra and Froelich, 2012; Pogge von Strandmann et al., 2021b; Ramos et al., 2022; Sproson et al., 2022; Wilson et al., 2021).

However, a few key unknowns remain in our interpretation of Li isotope behaviour during weathering. In particular, the partition coefficients and isotopic fractionation factors for different secondary minerals are not fully known. In addition, the distribution of Li removal between adsorption (the exchangeable fraction), and uptake into oxides and clays, is also uncertain, which matters because it is likely only the latter phase survives in archives such as detrital material. One of the primary methods available for characterising and quantifying these processes is through controlled laboratory weathering experiments. However, relatively few such studies have been completed (Hindshaw et al., 2019; Li and Liu, 2020; Pistiner and Henderson, 2003; Pogge von Strandmann et al., 2019b; Pogge von Strandmann et al., 2022a; Pogge von Strandmann et al., 2021c; Vigier et al., 2008; Wimpenny et al., 2015; Wimpenny et al., 2010; Zhang et al., 2025), especially in relation to studies of Li isotopes in the modern natural weathering environment.

In determining the Li uptake and isotopic fractionation during adsorption onto mineral surfaces, the exchangeable fraction in natural weathering has so far been shown to make up no more than ~10–15 % of the Li removed from solution, at least during basalt weathering (Pogge von Strandmann et al., 2019b; Pogge von Strandmann et al., 2022a). Therefore, methods are particularly needed to understand the effect of incorporation into clays. Generally, two different types of weathering experiments exist. The first approach aims to precipitate a single type of secondary mineral, in order to directly measure the isotopic fractionation factor (Hindshaw et al., 2019; Vigier et al., 2008). However, this mineral synthesis approach is challenging because most clay minerals are difficult, if not impossible, to precipitate artificially at low temperatures. The second approach subjects a natural and well-characterised rock to weathering in water, and allows a combination of different secondary minerals to form. While a fractionation factor for a single mineral is not obtained in such weathering experiments, they provide a fractionation factor relevant to the mixture of secondary minerals that form when a specific rock type is weathered (Pogge von Strandmann et al., 2019b; Pogge von Strandmann et al., 2022a).

Of the "natural weathering" experiments, there are a further two approaches. "Closed system" experiments react rock with water in a closed environment (albeit not for gases like CO_2). This design allows the relatively rapid supersaturation of the water, and hence the formation of secondary minerals. In such experiments using basalts, the observed fractionation factors were found to be identical to those reported from basaltic rivers (Pogge von Strandmann et al., 2019b; Pogge von Strandmann et al., 2022a), supporting their validity and relevance to natural systems. "Open system" experiments involve water being continuously dripped through the reacting rock. This design involves much larger volumes of water, meaning that such experiments have a higher water-rock ratio. The other key difference is the continuous addition of undersaturated water, and hence generally a longer period before steady-state is reached. Thus, even if the two types of experiment had the same water-rock ratio, it would be expected that the solutions in an open-system experiment would become supersaturated more slowly. Open system experiments may be expected to more closely mimic natural weathering scenarios, such as when rainwater seeps through soil profiles (Pogge von Strandmann et al., 2021c).

While both open and closed system approaches have been used, to date there has been no direct comparison between the two different types of weathering experiment for Li isotopes. Hence, it remains unknown how the results from the different types compare, and which are more representative of the processes that occur during natural (or enhanced) weathering, and therefore which are a better choice for future weathering experiments. In this study, open and closed system experiments were conducted using the same basalt (basanite) rock and water and are directly compared using both major elemental chemistry and Li isotopes, in order to facilitate the choice of future representative weathering experiments.

2. Methods

2.1. Experimental methods

The rock used for these experiments was the Eifelgold basanite, produced by Lava Union GmbH (https://www.rpbl.de), which effectively represents a Si-poor basalt. This material is commercially available as a crop fertiliser, and has been previously used for ERW experiments (Amann et al., 2022), including as one of the primary materials being used in the CarbDown enhanced weathering experiments (Germany's largest ERW scheme; https://www.carbon-drawdown.de). The surface area of the Eifelgold was measured via BET. The water used was groundwater from Mainz, Germany. The reason for using natural water, rather than artificial river water, is to achieve a natural charge balance, with reasonable amounts of alkalinity and chloride. Two replicates of each type of experiment were run, to assess experimental variability, although only samples from one experiment of each type were analysed for Li isotopes.

The closed experiments were effectively identical to others that have previously been run using different basaltic rocks (Pogge von Strandmann et al., 2019b; Pogge von Strandmann et al., 2022a). In these experiments 200 g of basanite powder was added to 900 ml of water, and then reacted in temperature-controlled shaking bath reactors at 21 °C for just over a month (Fig. 1). The solution was periodically sampled, with pH and temperature being recorded, and was then filtered at 0.2 μm and stored for analysis. The solids were sampled after the experiments finished, dried in an oven at 80 °C, and stored for comparison to the pre-reaction solids.

The open experiments also used 200 g of basanite powder, but in a column, and water was added at a rate of 3 ml/h via a peristaltic pump (Fig. 1). This drip rate into the column was tuned before the experiment to be identical to the drip rate out of the column, which was largely

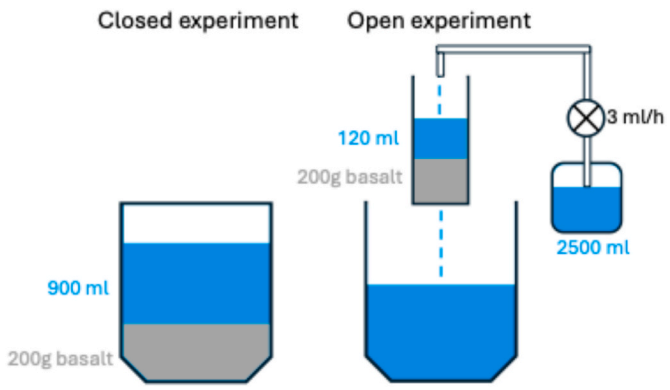

Fig. 1. Schematic of the two experiment types.

determined by the grain size of the reacting basanite. To ensure that the individual drips from the pump did not drip on the same place on the rock powder, and hence form preferential channels, a reservoir of 120 ml above the rock was added, which maintained its volume throughout the experiment due to the identical input and output flow rates. These experiments were also maintained at 21 °C for just over one month, which led to a water volume of just under 2500 ml being passed through the column. The accumulated water was sampled periodically, and the solids were sampled in the same way as for the closed system experiments.

2.2. Digestion and leaching methods

The initial Eifelgold basalt was digested following a standard dissolution procedure of HF–HNO_3–$HClO_4$, followed by HNO_3, and then HCl.

The exchangeable fraction in both the initial and post-experiment samples was preferentially leached using 1 M Na acetate for 1 h (Liu et al., 2022; Pogge von Strandmann et al., 2019b; Tessier et al., 1979), after which the samples were centrifuged, and the supernatant was pipetted off and dried down for isotope analysis.

The Eifelgold basalt was also leached for 1 h in 0.1 M HCl, in order to examine the most easily dissolved fraction.

2.3. Concentration analyses

The elemental concentrations of the filtered waters were analysed using an Agilent 8900 Triple-Quad ICP-MS at the University of Mainz. An on-line internal standard (Rh and In) was added to each sample and standard, to monitor and correct for instrumental drift. Water concentrations were established using a calibration line made from artificial element solutions, and accuracy and precision were monitored using the international river water standard SLRS-6. Rock analyses used the USGS standard BCR-2 for the same purpose. The analytical precision was ±3 % for both major and minor elements.

The major element concentrations, mineralogy and grain-size of the initial Eifelgold basalt have previously been reported (Amann et al., 2022).

2.4. Lithium isotope analysis

For the experimental waters, sufficient water was evaporated to obtain ~5 ng of Li, which was then purified through a two-column cation exchange procedure using AG50W X12 and 0.2 M HCl as the eluant, in the LOGIC laboratories at University College London. This procedure has been used in many previous studies (e.g. Pogge von Strandmann et al., 2019b). The same column procedure was used to purify the exchangeable leachates, and the digested initial basalt.

Analyses were performed on a Nu Plasma 3 MC-ICP-MS, also in the LOGIC laboratories at UCL, relative to the normalising standard IRMM-016, which is effectively identical to the LSVEC standard (Jeffcoate et al., 2004; Pogge von Strandmann et al., 2019b). Accuracy and precision for the solution samples were determined by repeated analysed of the IAPSO seawater standard, which over a period of 6 years yielded a δ^7Li value of 31.18 ± 0.38 ‰ (2sd, n = 52). The USGS BCR-2 basalt standard was also analysed, yielding δ^7Li values of 2.57 ± 0.30 ‰ (2sd, n = 11). Hence, the long-term external error of this procedure is conservatively ±0.4 ‰ (2sd).

3. Results

All data tables are provided in the Supplement. Major elemental concentrations of the initial water for the experiments are within the range of basaltic rivers (e.g. [Mg] = 21 μg/ml, compared to ≤ 10 μg/ml in Iceland (Gíslason et al., 1996) and ≤30 μg/ml in Reunion (Louvat and Allegre, 1997); [K] = 2.9 μg/ml compared to SW Icelandic rivers of ≤8.8 μg/ml (Gíslason et al., 1996), and in Reunion of ≤5 μg/ml (Louvat and Allegre, 1997)). Elemental ratios of this water are also similar to basaltic rivers (e.g. Mg/Na is 0.6 compared to a range of 0.14–1.02 in Icelandic rivers, while Ca/Na is 2.4, compared to 0.4–2.6 in Iceland (Gíslason et al., 1996; Louvat et al., 2008)).

The initial Li concentration of the experimental waters (~14 ng/ml) is slightly higher than in basaltic rivers (≤8 ng/ml in Icelandic and Reunion rivers (Louvat and Allegre, 1997; Louvat et al., 2008)), which may be because of the removal of Li that occurs during basaltic weathering, as examined in this study.

3.1. Closed experiments

As the two replicates of each experiment were effectively identical, the figures only show the data from one experiment of each type. In the closed experiment, the solution pH values increased from 7.6 in the original unreacted water to ~8.2 by the end of the experiments. Similarly to previous basaltic closed-system weathering experiments (Jones et al., 2012; Pogge von Strandmann et al., 2019b; Pogge von Strandmann et al., 2022a), the Na, Mg and Si concentrations increased by ~40 %, ~40 % and ~20 % respectively (Fig. 2). In contrast, Ca concentrations decreased by ~25 %. Other elemental concentrations, such as

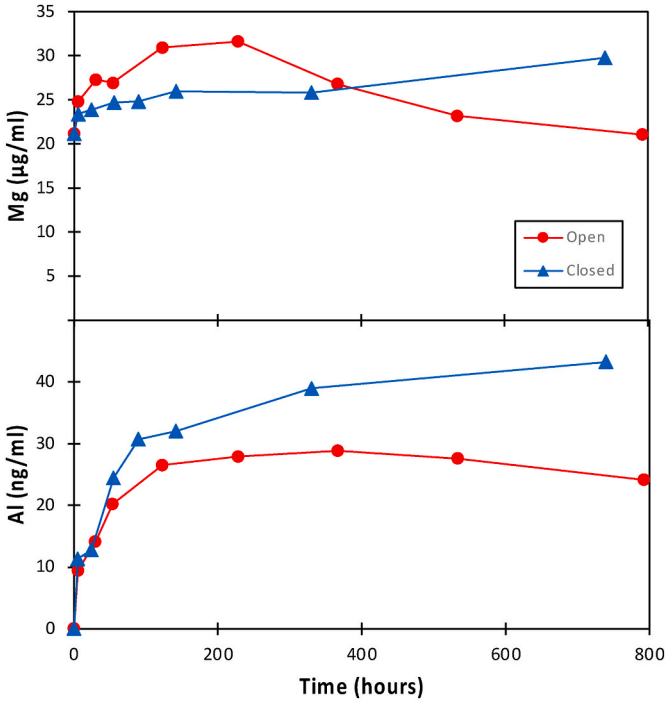

Fig. 2. Mg and Al concentrations in both experiments as a function of time.

those of Al, also increased (Fig. 2), but Fe concentrations slightly decreased.

Lithium concentrations decreased, as in all previous basaltic experiments, in this case from ~14 to 1.8 ng/ml. At the same time, the solution δ^7Li values increased, from 15.2 to 37.3 ‰ (Fig. 3).

The initial unreacted solid had an exchangeable δ^7Li value of 14.9 ‰, and the reacted solid in this experiment had an exchangeable δ^7Li value of 24.0 ‰. The total Li concentration of this phase was ~35 ng/g, which is ~7000 ng Li in total. Correcting for the exchangeable fraction of the initial unreacted basalt indicates that ~4740 ng Li was added to the exchangeable fraction throughout the experiment.

3.2. Open experiments

In the open experiment, the solution pH values evolved from an identical initial value of 7.6 to values of ~8.4. The solution concentration behaviour was more complex than in the equivalent closed experiments (Fig. 2). Major elements such as Na, Mg, K and Si tended to increase to a peak within ~200 h, and then decrease to concentrations similar to the initial values. Calcium concentrations behaved in the opposite manner, decreasing rapidly, and then increasing back to higher values. The concentrations of elements such as Al and Fe tended to increase through the experiment.

The Li concentrations of these experiments appear similar to those of the closed experiments, decreasing rapidly from the same starting point (~14 ng/ml) to 1.4 ng/ml by the end of the experiment, but with a faster initial decrease. The Li isotope composition also increased, reaching 29.5 ‰ by the end of the experiment, approximately 8 ‰ lower than in the closed experiments. This behaviour results in both types of experiment exhibiting negative co-variations between Li/Na ratios and δ^7Li, as also observed in other basaltic weathering experiments (Pogge von Strandmann et al., 2019b; Pogge von Strandmann et al., 2022a), natural basaltic weathering (Liu et al., 2015; Pogge von Strandmann et al., 2010; Pogge von Strandmann et al., 2006; Pogge von Strandmann et al., 2016; Pogge von Strandmann et al., 2021a; Pogge von Strandmann et al., 2023; Vigier et al., 2009), and also in the natural weathering of other lithologies (e.g. Dellinger et al., 2015; Murphy et al., 2019; Pogge von Strandmann et al., 2017).

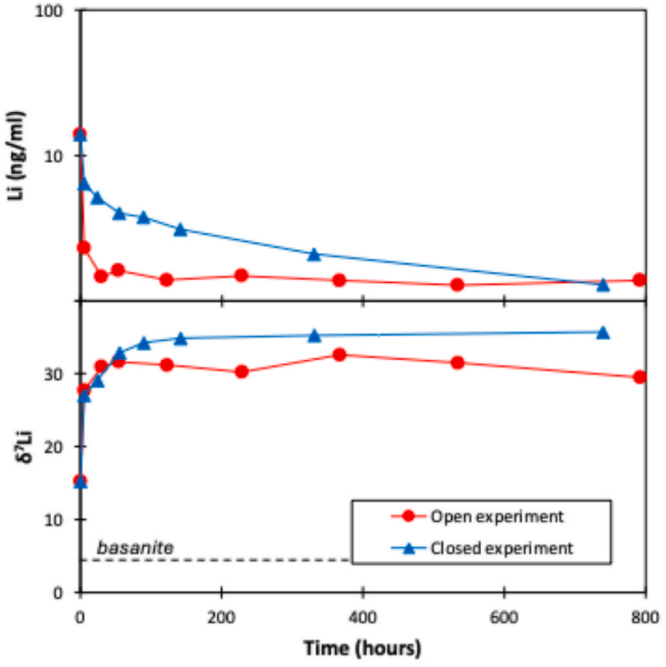

Fig. 3. Dissolved Li concentrations and isotopes in both experiments as a function of time. The values at time zero are the compositions of the initial water.

The exchangeable fraction of the reacted post-experimental solid had a Li concentration of ~87 ng/g, and a δ^7Li value of 24.3 ‰, and hence accumulated ~14,900 ng Li in the entire experiment (when corrected for Li in the exchangeable fraction of the initial basalt). The higher concentration of Li in this fraction, compared to the closed experiments, is likely because of the greater total water volume used.

4. Discussion

4.1. Mobility

The relative mobility of an element determines whether it preferentially goes into solution (mobile), or is retained by secondary minerals (immobile). Generally during natural basaltic weathering, Na is the most mobile major cation, and hence mobility is calculated relative to [Na], with the formula: $[x/Na]_{water}/[x/Na]_{rock}$ (Gíslason et al., 1996), where x is the element under investigation. In Icelandic or Azores basaltic rivers, K is generally similarly mobile to Na, while Mg, Ca and Li are approximately an order of magnitude less mobile, and elements such as Mn, Al and Fe are around two orders of magnitude below that (Gíslason et al., 1996; Pogge von Strandmann et al., 2010; Pogge von Strandmann et al., 2016; Pogge von Strandmann et al., 2021a).

Similar overall patterns are observed in these experiments with basanite, but there are differences between the experiments, despite the identical rock and initial water used. In the final sample of both experiments (approaching steady-state), the mobility order is K > Na > Ca > Mg > Li > Si ≫ Al, Fe, Mn. However, the relative mobility in the closed experiments is lower for every element (by a factor of 1–2) than in the open system experiments (Fig. 4). This result suggests that the elemental uptake by secondary minerals is greater in the closed experiments, but also that the mixture of secondary minerals is not significantly different between the experiments (i.e. the formation rate is different, but not the mineral type, as the relative abundance of elements in the solution does not change). This scenario makes sense, given that it is quicker and easier for a smaller volume of water to become supersaturated.

4.2. Mineral saturation behaviour

Mineral saturation indices (SI) were calculated using the PHREEQC programme (Parkhurst and Appelo, 1999), with elemental concentrations, pH and temperature as inputs, and with the addition of the THERMODDEM and MINTEQ thermodynamic databases. In both experiment types, the main primary minerals (forsterite, plagioclase, pyroxene) were similarly undersaturated (Fig. 5), suggesting that these minerals were dissolving throughout the experiments. The typical basaltic secondary minerals (smectite, kaolinite and Fe-oxyhydroxides

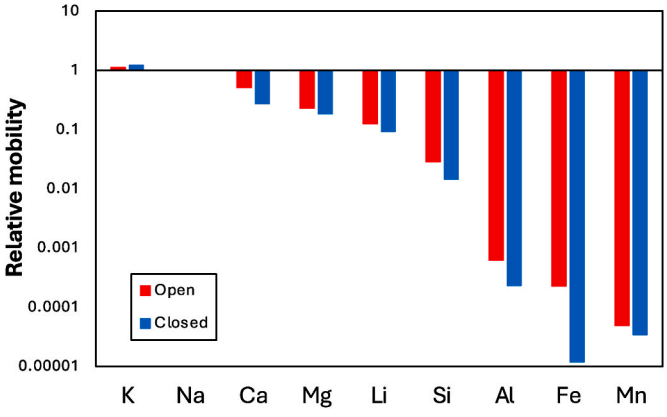

Fig. 4. Elemental mobility for a range of elements relative to Na (Gíslason et al., 1996) for each experiment type.

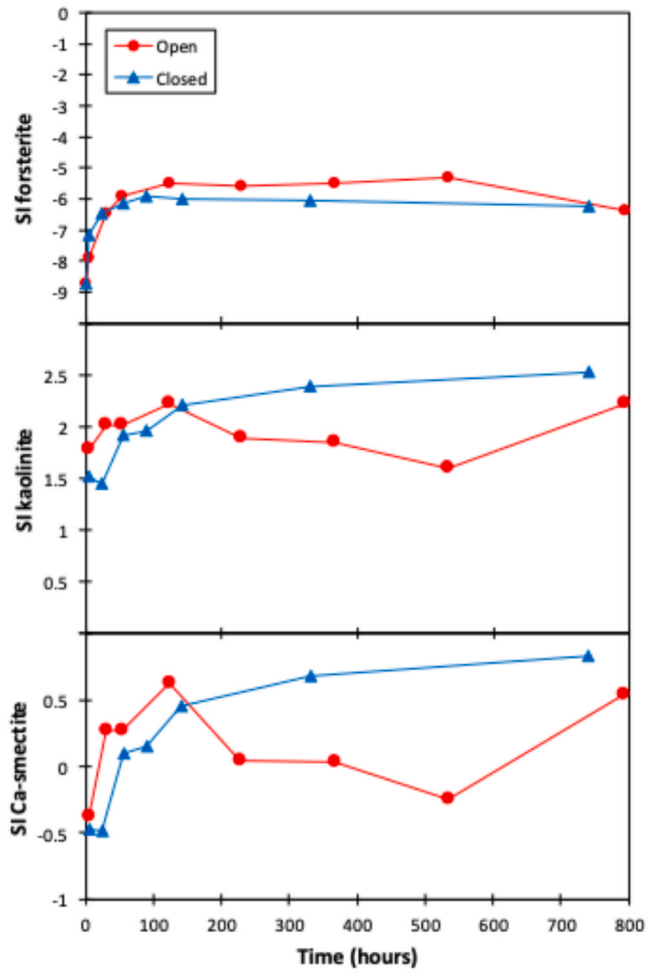

Fig. 5. Saturation index (SI) for selected primary (olivine) and secondary (kaolinite, smectite) minerals in both experiments as a function of time.

such as goethite and ferrihydrite, as well as poorly crystalline or amorphous allophane and imogolite (Stefansson and Gislason, 2001)) were all supersaturated, implying that the precipitation of these minerals was feasible, generally with the degree of supersaturation increasing with time (Fig. 5). We note that the initial versions of the precipitating minerals were likely amorphous precursors, rather than fully crystalline clays (Pogge von Strandmann et al., 2019b).

In the final samples of each experiment type (i.e. those closest to steady-state), while the secondary mineral supersaturation levels were similar, the saturation indices were consistently higher in the closed experiments (by factors of ~1.5–2; Fig. 5). This result implies that secondary mineral formation was likely higher in the closed compared to the open experiments, supporting the idea that the more limited volume of water would become more easily supersaturated, and in agreement with the observed differences in elemental mobilities (Fig. 4).

4.3. Major element behaviour

While the elemental mobility and saturation indices suggest secondary silicate mineral formation, the formation of secondary carbonates appears not to play a significant role in either experiment. In general, Ca/Sr ratios are often considered as an indicator of carbonate precipitation, because the Ca/Sr ratio of carbonates is high (higher than the ratio of basalts, with molar ratios of up to 4000), and hence carbonate formation will drive the Ca/Sr of waters towards lower values (e.g. Jacobson et al., 2015; Jacobson and Blum, 2000; Pogge von Strandmann et al., 2019c). Here, the Ca/Sr ratio in both experiments increases with time, indicative of dissolving basalt (with Ca/Sr ~ 890). However, the pattern of the Ca/Sr increase is different between the two experiment types (Fig. 6): in the open system experiments, the Ca/Sr continuously increases (Fig. 6), and never reaches an apparent equilibrium (i.e. ratio steady-state), whereas the closed system experiment reaches a steady-state after ~400 h.

The same picture arises when examining elements that are involved in secondary silicate mineral formation. For example, the comparison of mobile/immobile element ratios, such as Al/K, shows a continuous increase towards (but not close to reaching) the high value of basalt (~2.7) in the open experiment, while the closed experiment rapidly reaches a plateau (Fig. 6). This plateau implies that secondary minerals containing both K and Al started precipitating, and that a dynamic steady-state condition is much more rapidly reached in the closed experiment than in the open one. This finding is as expected because a smaller volume of water should more rapidly reach both saturation and steady-state (equilibrium) more rapidly. In other words, major elemental behaviour reaches equilibrium between dissolution and precipitation significantly more rapidly in a closed experiment than in an open one, likely due to the continuous addition of undersaturated water in the latter case.

4.4. Trace element behaviour

Part of the interest, and concern, regarding the possible widespread use of enhanced weathering reactions is the potential for the release of critical micro-nutrients (e.g. Cu, Zn) and/or toxic heavy metals (e.g. Ni, Cd, Co). Experiments like those conducted here may help to determine the release rates and fate of such metals that could be sourced from the dissolution of basalt. Several of these elements, as well as their isotopes, are also used to study natural systems in waters, such as nutrient supply or organic matter behaviour (e.g. Cu, Zn, Ba; Horner and Crockford, 2021; Little et al., 2019).

For all the elements mentioned above, the solution concentration decreases throughout both experiment types. For example, Ba concentrations decrease by an order of magnitude, and Ni by more than a factor of 3 (Fig. 7). This pattern strongly suggests that they are being taken up by (silicate) secondary minerals during the inorganic weathering

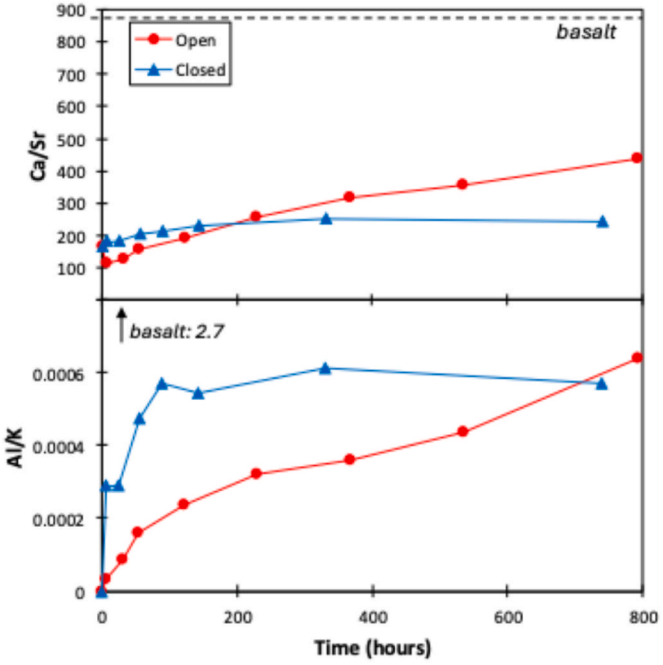

Fig. 6. Elemental ratios (Ca/Sr and Al/K) in both experiments as a function of time.

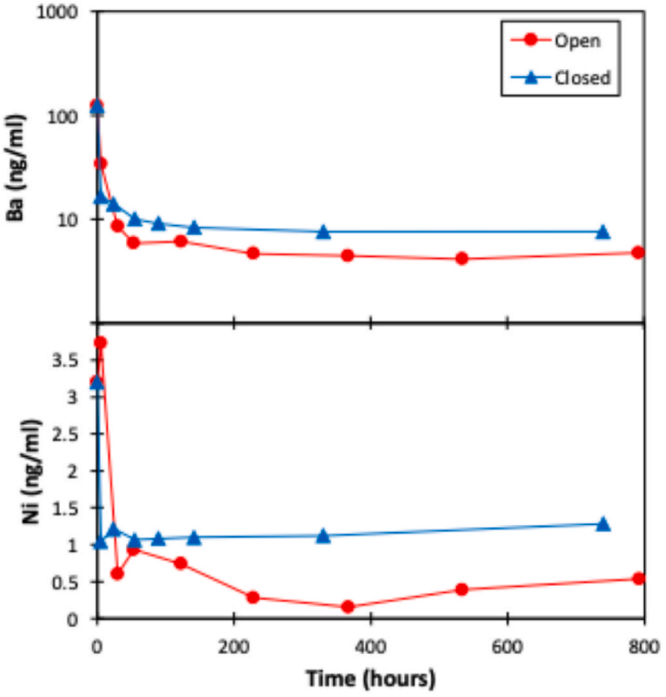

Fig. 7. Ba and Ni concentrations in both experiments as a function of time.

process.

For enhanced weathering applications, the implication of this removal process is that it is less likely that drinking water thresholds for these metals will be breached, which is in agreement with previous enhanced weathering experiments and studies (e.g. Haque et al., 2020; Iff et al., 2024; Pogge von Strandmann et al., 2022b; Renforth, 2012; Renforth et al., 2015). However, it is suggested that plants obtain a significant proportion of their nutrients from the soil exchangeable fraction (i.e. adsorbed to the surface of secondary minerals), or even leach them from clays (e.g. Steinhoefel et al., 2021). Hence, if large proportions of the toxic heavy metals are taken up by these fractions, it could lead to the solid fraction of soils eventually breaching safety guidelines, especially with repeated applications of amendment rock (Iff et al., 2024).

For the examination of natural systems, the implication is that the cycling of these elements (and their isotopes) may also be strongly controlled by the specifics of the inorganic weathering process, including adsorption and secondary mineral formation processes. Therefore, these effects may need to be disentangled, especially if these systems are being used to reconstruct past changes in natural processes.

4.5. Rock dissolution

In previous basaltic water-rock interaction experiments (Jones et al., 2012; Pogge von Strandmann et al., 2019b; Pogge von Strandmann et al., 2022a), the major element concentrations (e.g. Na, K, Mg, Si) were used to determine the amount of basalt dissolution. This calculation assumes that those elements are insignificantly affected by secondary mineral formation. In the case of the closed experiment, the solution concentration must be corrected for the decrease in water volume due to sampling to calculate the elemental mass, and then compared to the theoretical elemental mass change that would have occurred if only the water volume but not the concentration had changed. Then, using the elemental concentrations of the Eifelgold basalt, the amount of basalt nominally dissolved can be calculated.

In the closed experiment, based on Na concentrations, ~0.5 g of basalt was dissolved. Based on Mg concentrations, this figure is ~0.1 g, implying that Mg has been removed from solution into secondary minerals, as also shown by Mg having ~5 times lower mobility than Na in these experiments (Fig. 4). The concentrations of K, the most mobile major cation here, in the bulk basalt suggest that ~1.9 g of basalt was dissolved, which would be a dissolution rate of ~0.06 g/day. This behaviour of K agrees with other experiments using the Eifelgold basinite, and was attributed to the abundance of nepheline [$Na_3KAl_4Si_4O_{16}$] (Amann et al., 2022), a feldspathoid that is common in the Eifel region, and which has higher dissolution rates than other Na-dominated rock-forming minerals (Lasaga et al., 1994).

This calculation is more difficult for the open system experiments, because both [Na] and [Mg] are lower by the end of the experiments than at the start (Fig. 2), although both reach a peak early in the experimental run. This deficit remains when correcting the mass balance for the amount of the relevant element continuously added through the input solution, implying that Na and Mg are being removed into secondary phases or the exchangeable fraction. The precise reason for this difference from the closed experiments needs to be investigated further. However, using the K concentrations would suggest that ~3.2 g of basalt was dissolved (a rate of ~0.09 g/day). This is further discussed below in terms of the mass balance.

From the above calculations, two aspects become clear: i) the different experiment types lead to different amounts of basalt dissolution, with faster dissolution in the open experiments; ii) given apparently variable dissolution and precipitation, a single diagnostic element to quantify basalt dissolution does not exist. This example highlights one key reason why isotope geochemistry has often taken the forefront in weathering studies.

4.6. Lithium mass balance

Although aspects of the two types of experiments appear similar, such as their general Li behaviour, the mass balances of Li are very different. For the closed experiments, the Li available at the start of the experiment is that contained within the initial 900 ml of water. Lithium is then removed from solution into secondary phases and the exchangeable fraction, as demonstrated in previous similar basaltic weathering experiments (Jones et al., 2012; Pogge von Strandmann et al., 2019b; Pogge von Strandmann et al., 2022a). The mass balance calculations at each step therefore have to take into account the decrease in solution volume due to sampling; thus, the initial solution contained ~12,500 ng of Li, which decreased to ~940 ng by the end of the experiment. Such a loss of almost 93 % of dissolved Li is comparable to previous basaltic experiments, where 82–87 % of dissolved Li was lost. In the case of both experiments, the dissolution of ~1.9–3.2 g of basalt would imply that on the order of 10,000 ng of Li were added to solution by rock dissolution. However, this process is not observed in mixing diagram, where solution Li isotope ratios follow removal trends with no resolvable trend towards higher [Li] and lower δ^7Li that would be expected from the addition of Li from bulk rock dissolution (Fig. 8). Hence, it seems likely that the amount of Li removed was significantly larger than the amount added by dissolution. We therefore conclude that the addition of K during rock dissolution is from incongruent dissolution of a K-rich, Li-poor mineral (likely nepheline).

This hypothesis was further investigated by leaching the Eifelgold in 0.1 M HCl for 1 h. The Li/K mass ratio of the leach is $\sim 5 \times 10^{-5}$, while the Li/K ratio of the bulk basanite is $\sim 3 \times 10^{-4}$. The Li/K ratio of the reacted waters rapidly reaches a plateau at a similar value to the leach of $\sim 3 \times 10^{-5}$. Thus, it appears that the earliest dissolution of the rock releases K, but not much Li, which is likely why the Li removal trends detailed below (Section 4.7) exhibit no obvious Li addition by dissolution. Hence, Li addition by dissolution is an insignificant factor in our Li budget and is not accounted for here. In other words, the solids must have gained ~11,600 ng of Li during the course of the experiment.

Of the Li lost to the solids, the exchangeable leach suggests that ~41 % of the Li went into the exchangeable fraction. This proportion is higher than in the previous basaltic weathering experiments, where

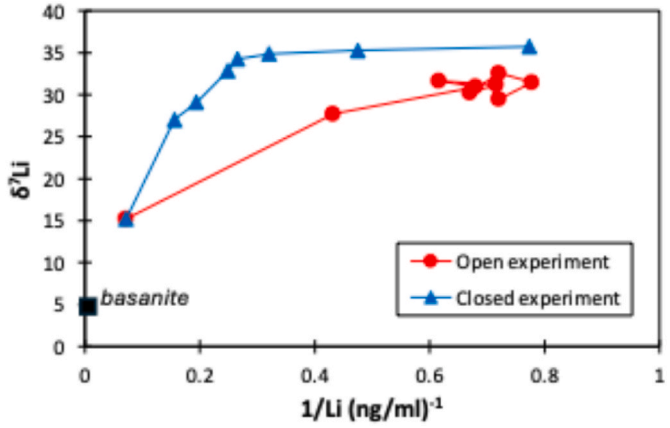

Fig. 8. Dissolved Li isotopes as a function of Li concentrations. Error bars are smaller than the symbol sizes.

<16 % went into the exchangeable fraction. This difference is unlikely to be due to the grain size, because the values are similar (Eifelgold: 3.1 m^2/g; Borgarfjörður sand in previous publications: 3.88 m^2/g). The likely key difference between the two basalts is likely that the Eifelgold is freshly quarried and ground, while the Borgarfjörður sand was collected from a river bank, and is therefore already weathered. Hence, the fresher surfaces in the Eifelgold could provide more potential sites for cation exchange. However, this idea requires further testing.

In the open system experiment, the mass balance is more complex, because water containing ~14 ng/ml Li was continuously added to the experiment. In total, 34,800 ng of Li was introduced during the course of the experiment. The decreasing Li concentration of the reacting water means that a total of ~3470 ng of Li actually made it through the column, which means that ~91 % of dissolved Li (~31,300 ng) was removed into solid phases. The water/rock ratio of these experiments was 12.5, significantly higher than the closed experiments (4.5 at the start of the experiment).

In this experiment, ~48 % of the Li lost from solution was taken up into the exchangeable fraction. This proportion is similar to the proportion in the closed experiment (~41 %), which suggests that grain freshness, rather than the experiment type, could be a major controlling factor.

4.7. Lithium isotope fractionation

In both experiments, the exchangeable fraction removed a similar proportion of the Li from solution, despite the quite different amounts of Li added from the solutions. However, the fractionation into that fraction, based on the final solution δ^7Li value, differed between the experiments. For the closed experiment, the $\Delta^7Li_{exch\text{-}soln}$ was −11.7 ‰, indistinguishable from previous (closed) basalt weathering experiments (Pogge von Strandmann et al., 2019b). Assuming that the remainder of the Li was removed into secondary minerals (oxides + clays), and that equilibrium was reached, this implies a fractionation of $\Delta^7Li_{secmin\text{-}soln}$ = −26.6 ‰. This value is similar to, but slightly larger than, the −22.5 to −23.9 ‰ fractionation inferred from the previous experiments. This small difference could be a function of the different rock type (basalt versus basanite), and hence some differences in the secondary minerals that formed.

In contrast, in the open experiment, $\Delta^7Li_{exch\text{-}soln}$ was −5.2 ‰, and the cumulative secondary minerals can be inferred to have exerted a fractionation of $\Delta^7Li_{secmin\text{-}soln}$ = −14.3 ‰. The lower fractionation of both the exchangeable fraction and the combined secondary minerals is likely due to the lower water-rock interaction time in the open experiments. A number of studies have shown that the dissolved δ^7Li values in natural systems depend on the water-rock interaction time, for example by comparison to fluid drip rates or riverine discharge, with δ^7Li values decreasing as interaction time decreases (Golla et al., 2022; Pogge von Strandmann et al., 2023; Wilson et al., 2021; Zhang et al., 2022). In basaltic river suspended loads, the magnitude of Li isotope fractionation between the exchangeable or clay fraction and water also decreases as interaction time decreases (Pogge von Strandmann et al., 2023). Therefore, the lower fractionation for both the exchangeable fraction and secondary minerals for the open experiment, where the water-rock interaction time is significantly shorter, is consistent with those studies, and provides independent experimental verification.

Although more than twice the amount of Li was removed from solution in the open experiment compared to the closed experiment, and more Li was also added because of the higher water volume, the dissolved Li isotope behaviour was broadly similar between the two experiments (Fig. 3). However, there are differences in the relationship between [Li] and δ^7Li in the experiments (Fig. 8), with different δ^7Li values achieved once relatively constant [Li] is reached. Fig. 8 also demonstrates that no significant Li was added from rock dissolution, as that would drive solution [Li] higher, and δ^7Li lower.

In both types of experiments, similar trends are observed in δ^7Li values versus Li/Na ratios occur (Fig. 9), and the negative relationships between these two parameters implies that Li is being removed into or onto secondary phases. While the relatively narrow ranges in δ^7Li values for most of the experimental waters make it difficult to determine exactly which fractionation law is being following, the closest match for both experiments is to an equilibrium (batch) fractionation relationship, due to the relatively constant δ^7Li values with changing Li/Na ratios towards the ends of each experiment (Fig. 9). This result is in contrast to previous basaltic experiments, where a Rayleigh fractionation relationship was better able to explain the data (Pogge von Strandmann et al., 2019b; Pogge von Strandmann et al., 2022a).

The difference in fractionation behaviour between these experiments and those conducted previously may be due to a lack of previously formed secondary minerals and the presence of significant fresh surfaces due to grinding in the Eifelgold. In contrast, the previous experiments used weathered river sands, which were not ground, and hence surfaces were likely at least partly covered by secondary minerals (Jones et al., 2012). Such differences likely drove faster reaction rates in the Eifelgold.

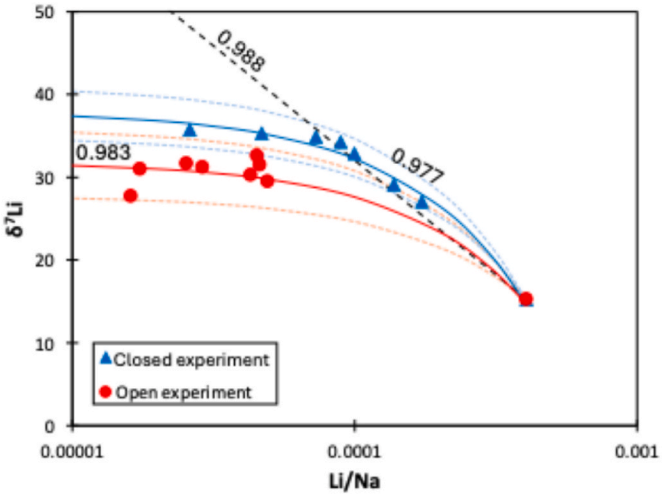

Fig. 9. Dissolved Li isotopes versus Li/Na ratios, indicating Li isotope fractionation behaviour. The curved lines represent equilibrium fractionation paths, with the solid lines corresponding to the best-fit mean, and the lighter dashed colours representing the upper and lower uncertainty bounds. The dashed black line is an example of a Rayleigh fractionation pathway, showing how such a pathway does not fit these data. The numbers correspond to the α value for the main pathways. Error bars for Li isotopes are smaller than the symbol sizes. (For interpretation of the references to colour in this figure legend, the reader is referred to the Web version of this article.)

Therefore, these faster-reacting experiments could have evolved more quickly towards true equilibrium than the previous slower-reacting experiments, leading to Li isotope fractionation behaviour that is better described by equilibrium fractionation. This effect is also observed in river waters from the Amazon Basin, where settings with faster-reacting fresh rocks tend to follow equilibrium fractionation, whereas slower-reacting older rocks tend to drive a Rayleigh fractionation trend (Maffre et al., 2020).

Assuming that equilibrium fractionation appropriately describes these experiments, the best-fit fractionation factor for the closed experiment is $\alpha = 0.977 \pm 0.003$, and for the open experiment is $\alpha = 0.983 \pm 0.004$ (Fig. 9), where the uncertainty is based on the error in the regression fit. These values are similar to fractionation factors of ~0.98 observed during the alteration of the oceanic crust (Chan et al., 1992), and basalt particles in estuaries (Pogge von Strandmann et al., 2008), as well as a series of clay formation experiments: $\alpha = 0.9812$ (Vigier et al., 2008), 0.9813 (Millot et al., 2010), 0.9834 (Hindshaw et al., 2019), and theoretical calculations of $\alpha = 0.9828$ (Dupuis et al., 2017).

With a "known" fractionation factor, a starting Li isotope composition, and the measured solution Li isotope composition, it is possible to calculate the fraction of Li left in solution and that taken up into secondary minerals using standard stable isotope formulae (Pogge von Strandmann et al., 2019a; Pogge von Strandmann et al., 2019c; Vigier et al., 2009). Given the arguments above, we use an equilibrium fractionation formula and alpha value. It is then possible to calculate the concentration of Li taken into the secondary minerals, using the solution Li concentration and a partition coefficient. Here we examine the use of two different coefficients: 1) the experimental smectite partition coefficient from Decarreau et al. (2012), the only study to experimentally examine this process, based on their relationship between $D_{clay/solution}$, temperature and solution concentration, of D ~ 26.04 (Decarreau et al., 2012); 2) the partition coefficient directly from these experiments, based on the measured Li mass balance (i.e. Li removed from solution relative to that remaining in solution), of D ~9.04 for the open experiments, and D ~12.4 for the closed experiments. As well as uptake into clays, the latter partition coefficients will also include uptake into the exchangeable and oxide fractions. Note also that they directly stem from reactions at room temperature, whereas the experiments of Decarreau et al. (2012) were conducted at higher temperature, and then extrapolated by that study to lower temperatures. The equations are:

$$f_{water} = \frac{\delta - \delta_i}{1000\ ln\ \alpha} + 1 \quad \text{Eqn. 1}$$

$$f_{clay} = 1 - f_{water} \quad \text{Eqn. 2}$$

$$[Li]_{clay} = \left(\frac{[Li]_{water}}{f_{water}} \times f_{clay} \right) D \quad \text{Eqn. 3}$$

where f is the fraction of Li in that phase, and δ is the δ^7Li value (subscript i is the initial value).

The [Li] (Li concentration in the water or clay; Eqn. (3)) can then theoretically be converted to a total mass of Li in the secondary minerals by using the initial mass of the basalt from the start of the experiment (in this case 197.3 g). This assumes that most of the elements in the clay stem from the basalt. This approach assumes that all the basalt in the reactor had contact with the drip water, which may not be entirely correct for the open-system experiment, and hence it would be a maximum estimate. This calculation, based on the fluid Li isotope ratios, suggests that ~28,500 ± 2500 ng of Li was removed into secondary minerals in the open experiments (using the lower $D_{clay/solution}$ based on our experiments), which is remarkably close to the ~31,300 ng calculated via the concentration-based mass balance (see above). In other words, Li removal amounts based on isotopic fractionation appear to be fairly accurate. Using the higher value of D for smectite (Decarreau et al., 2012), this value would be ~82,000 ± 7200 ng according to Eqn. (3), which appears significantly too high, and may be because part of the removal was into the exchangeable fraction with a lower fractionation factor (Pogge von Strandmann et al., 2020). Note that the uncertainty in these values is the propagated 2sd uncertainty in the analyses of the values of α, δ^7Li, [Li], D and the basalt mass.

Calculating the actual amount of clay that forms clearly depends on "knowing" the Li concentration of the clay, which in turn requires clay synthesis experiments, such as those of Decarreau et al. (2012) or Hindshaw et al. (2019). The former study provides a relationship between solution and clay concentration, but only at a lowest temperature of 75 °C. Using this relationship and our solution [Li] suggests that up to 46 g of clay could form, which is likely too high (i.e. 23 % of the ~200 g of basalt reacted), given how little basalt appears to have dissolved. Hindshaw et al. (2019) synthesised clays at 20 °C, and using their longest-reacted clay concentration of ~7 μg/g, the open experiments suggest approximately 4.0 g of clay formed during the reaction of 200 g of basalt (i.e. ~2 % of basalt reacted) during a month.

Applying the same calculation to the closed experiments, using our experimental $D_{clay/solution}$ value, suggests that 13,000 ± 1100 ng of Li was removed into clays, which compares well to the estimate of ~11,600 ng from the mass balance approach. Using the clay Li concentrations of Hindshaw et al. (2019), it which would equate to ~1.8 g of clay (1 % of basalt reacted).

Interestingly, the above calculations would imply less secondary mineral formation per amount of basalt in the closed experiments, which could appear to be in contrast to the evidence mentioned above (i.e. saturation indices, major elements, mobility, solution δ^7Li). This difference is effectively because more water passed through the open experiments, and both the mass balance and the chemical reaction are at least partially dependent on the amount of water. Hence, if calculated relative to the amount of water used in each experiment, it equates to ~1.6 ± 0.2 g of clay per litre of water for the open-system experiments, and ~2.0 ± 0.3 g/l for the closed experiments. In other words, based on this quantification method, the open-system experiments appear to form more secondary minerals per unit of rock, but less per unit of water.

The significant point of these calculations is that it is possible to reliably (here within ~12 % of the mass balance value) calculate the amount of Li removed from water by secondary mineral formation based on the solution Li isotope composition and concentration. With a partition coefficient, it is then also possible to calculate the mass of Li taken into clays, and with a "known" clay concentration therefore also the amount of secondary minerals formed. Therefore, in the context of natural or enhanced weathering, it may be feasible to quantitatively determine clay formation from δ^7Li measurements. Importantly, for any given rock-water system, these calculations require a "known" isotopic fractionation factor and partition coefficient. Such parameters could be determined by conducting similar experiments to this study using the specific weathering materials of interest, thereby enabling the quantitative determination of clay formation in field locations.

Such a possibility of constraining clay formation could be particularly important for enhanced weathering reactions, where the uptake of cations by clay formation and adsorption will reduce the efficiency of CO_2 drawdown (because the cations necessary for carbonate formation and alkalinity charge balance are retained within clays) (Pogge von Strandmann and Henderson, 2015). Clays can also be important in terms of surface passivation, where they form on the surface of reactive silicates, thus slowing the reaction rates (Beerling et al., 2020). However, clay formation is generally hard to measure, given that there are no diagnostic elemental signals. As shown here, Li isotopes could potentially provide a route to quantify secondary mineral formation.

The data from these experiments suggest that, firstly, the mass of rock dissolution and clay formation approximately balance. This would generally be expected, given that clay precipitation is required to continue to dissolve primary minerals (e.g. Stefansson and Gislason, 2001). Secondly, the formation of clays is rapid. There is a tendency, especially in enhanced weathering, to assume that clay formation is too slow to impact ERW, largely because of studies based on elemental

concentrations. However, studies based on Li (e.g. Pogge von Strandmann et al., 2023), Mg (e.g. Oelkers et al., 2019) and Si (e.g. Geilert et al., 2023) isotopes show that clays can form within weeks during natural weathering. While rates are typically faster during laboratory experiments than in the field, this study (together with the natural studies mentioned above) shows that clays are a factor that must be considered even in single year ERW applications.

5. Conclusions

This study set out to compare open (drip-through) and closed system weathering experiments, especially for their Li isotope behaviour. In terms of general elemental behaviour, the overall patterns are similar. However, often the concentrations in the closed experiments appear to reach an equilibrium value fairly rapidly, while in the open experiments there is more variation. These differences lead to small variations in calculated elemental mobility and saturation indices, whereby the closed experiment has higher secondary mineral saturation by the end of the experiment, and slightly lower mobility of most cations than in the open experiment. This implies more (or faster) secondary mineral formation in the closed experiments, which is to be expected, given that it is easier to supersaturate a smaller volume of water. Whether this effect is directly due to the higher water-rock ratio of the open experiments, or more indirectly due to the continuous addition of undersaturated water, is unclear at this point, and more experiments are needed to resolve this question.

The experiments also show similarities and differences in Li isotope behaviour, with dissolved δ^7Li values increasing throughout both experiments, but finishing at slightly higher values in the closed experiments ($\delta^7Li = 35.7$ ‰) versus the open experiments ($\delta^7Li = 29.5$ ‰). The δ^7Li values in both experiment types appear to reach a steady-state value at similar rates (within ~100 h). However, the Li concentrations in the experiments continue to decrease after attaining approximately constant δ^7Li values, showing that both experiments can be explained by an equilibrium fractionation trend, whereby concentrations can change without significant concomitant changes in δ^7Li values.

The two types of experiment also yield Li isotope fractionation factors that are within uncertainty of each other ($\alpha = 0.983 \pm 0.004$ and 0.977 ± 0.003 for the open and closed experiments, respectively), which are also indistinguishable from fractionation factors calculated for the alteration of the basaltic oceanic crust (Chan et al., 1992), or of basalt particles in an estuary (Pogge von Strandmann et al., 2008). Hence, the two experiments show evidence of (very slightly) variable equilibrium fractionation factors, but also different fractions of Li removal, leading to different final solution δ^7Li values.

We also demonstrate that fractionation factors and partition coefficients from experiments such as these can reasonably be used to quantify secondary mineral formation in experimental and perhaps also natural settings, which may be particularly useful for studying enhanced weathering reactions in field settings. In the case of these experiments, we estimate that ~1.6 ± 0.2 g of clay per litre of water for the open system experiments, and ~2.0 ± 0.3 g/l for the closed experiments formed within one month, representing approximately 1 % of the initial mass of basalt. This mass is similar to the amount of basalt dissolved (1.9–3.2 g, based on K concentrations and assuming congruent dissolution), meaning that a significant proportion of dissolved material was rapidly taken up into or onto secondary minerals.

CRediT authorship contribution statement

Philip A.E. Pogge von Strandmann: Writing – review & editing, Writing – original draft, Project administration, Investigation, Funding acquisition, Formal analysis, Conceptualization. **Xiaoqing He:** Writing – review & editing, Investigation. **Ying Zhou:** Writing – review & editing, Conceptualization. **David J. Wilson:** Writing – review & editing, Investigation.

Declaration of competing interest

The authors declare that they have no known competing financial interests or personal relationships that could have appeared to influence the work reported in this paper.

Acknowledgements

Carolin Berg and Regina Walter are thanked for the concentration and BET measurements. PPvS and the isotope analyses were supported by ERC grant 682760. The CarbDown project is thanked for the initial motivation for this study. DJW was supported by a Natural Environment Research Council independent research fellowship (NE/T011440/1). For the purpose of open access, the author has applied a 'Creative Commons Attribution (CC BY) licence' to any Author Accepted Manuscript version arising. The first author interpreted and wrote this paper exclusively while sitting at the side of his children's sporting practices, and acknowledges his boredom. Two anonymous reviews are thanked, as well as careful editing by Jiubin Chen.

Appendix A. Supplementary data

Supplementary data to this article can be found online at https://doi.org/10.1016/j.apgeochem.2025.106458.

Data availability

Data are provided in the Supplement

References

Amann, T., Hartmann, J., Hellmann, R., Pedrosa, E.T., Malik, A., 2022. Enhanced weathering potentials—the role of in situ CO2 and grain size distribution. Front. Clim. 4.
Beerling, D.J., Kantzas, E.P., Lomas, M.R., Wade, P., Eufrasio, R.M., Renforth, P., Sarkar, B., Andrews, M.G., James, R.H., Pearce, C.R., Mercure, J.-F., Pollitt, H., Holden, P.B., Edwards, N.R., Khanna, M., Koh, L., Quegan, S., Pidgeom, N.F., Janssens, I.A., Hansen, J., Banwart, S.A., 2020. Potential for large-scale CO2 removal via enhanced rock weathering with croplands. Nature 583, 242–248.
Berner, R.A., 2003. The long-term carbon cycle, fossil fuels and atmospheric composition. Nature 426 (6964), 323–326.
Bouchez, J., von Blanckenburg, F., Schuessler, J.A., 2013. Modeling novel stable isotope ratios in the weathering zone. Am. J. Sci. 313.
Chan, L.H., Edmond, J.M., Thompson, G., Gillis, K., 1992. Lithium isotopic composition of submarine basalts: implications for the lithium cycle in the oceans. Earth Planet Sci. Lett. 108 (1–3), 151–160.
Clergue, C., Dellinger, M., Buss, H.L., Gaillardet, J., Benedetti, M.F., Dessert, C., 2015. Influence of atmospheric deposits and secondary minerals on Li isotopes budget in a highly weathered catchment, Guadeloupe (Lesser Antilles). Chem. Geol. 414, 28–41.
Decarreau, A., Vigier, N., Pálková, H., Petit, S., Vieillard, P., Fontaine, C., 2012. Partitioning of lithium between smectite and solution: an experimental approach. Geochem. Cosmochim. Acta 85, 314–325.
Dellinger, M., Gaillardet, J., Bouchez, J., Calmels, D., Louvat, P., Dosseto, A., Gorge, C., Alanoca, L., Maurice, L., 2015. Riverine Li isotope fractionation in the Amazon River basin controlled by the weathering regimes. Geochem. Cosmochim. Acta 164, 71–93.
Dupuis, R., Benoit, M., Tuckerman, M.E., Méheut, M., 2017. Importance of a fully anharmonic treatment of equilibrium isotope fractionation properties of dissolved ionic species as evidenced by Li+(aq). Acc. Chem. Res. 50, 1597–1605.
Elliott, T., Thomas, A., Jeffcoate, A., Niu, Y.L., 2006. Lithium isotope evidence for subduction-enriched mantle in the source of mid-ocean-ridge basalts. Nature 443 (7111), 565–568.
France-Lanord, C., Derry, L.A., 1997. Organic carbon burial forcing of the carbon cycle from Himalayan erosion. Nature 390 (6655), 65–67.
Geilert, S., Frick, D.A., Garbe-Schönberg, D., Scholz, F., Sommer, S., Grasse, P., Vogt, C., Dale, A.W., 2023. Coastal El Niño triggers rapid marine silicate alteration on the seafloor. Nat. Commun. 14 (1), 1676.
Gíslason, S.R., Arnorsson, S., Armannsson, H., 1996. Chemical weathering of basalt in southwest Iceland: effects of runoff, age of rocks and vegetative/glacial cover. Am. J. Sci. 296 (8), 837–907.
Golla, J.K., Bouchez, J., Kuessner, M.L., Rempe, D.M., Druhan, J.L., 2022. Subsurface weathering signatures in stream chemistry during an intense storm. Earth Planet Sci. Lett. 595, 117773.
Grimm, C., Martinez, R.E., Pokrovsky, O.S., Benning, L.G., Oelkers, E.H., 2019. Enhancement of cyanobacterial growth by riverine particulate material. Chem. Geol. 525, 143–167.
Haque, F., Chiang, Y.W., Santos, R.M., 2020. Risk assessment of Ni, Cr, and Si release from alkaline minerals during enhanced weathering. Open Agric. 5, 166–175.

Hartmann, J., West, A.J., Renforth, P., Kohler, P., De la Rocha, C.L., Wolf-Gladrow, D.A., Durr, H.H., Scheffran, J., 2013. Enhanced chemical weathering as a geoengineering strategy to reduce atmopsheric carbon dioxide, supply nutrients, and mitigate ocean acidification. Rev. Geophys. 51, 113–150.
Hindshaw, R.S., Tosca, R., Gout, T.L., Farnan, I., Tosca, N.J., Tipper, E.T., 2019. Experimental constraints on Li isotope fractionation during clay formation. Geochem. Cosmochim. Acta 250, 219–237.
Horner, T.J., Crockford, P.W., 2021. Barium isotopes: drivers, dependencies, and distributions through space and time. Elements in Geochemical Tracers in Earth System Science. Cambridge University Press, Cambridge.
Huh, Y., Chan, L.H., Zhang, L., Edmond, J.M., 1998. Lithium and its isotopes in major world rivers: implications for weathering and the oceanic budget. Geochem. Cosmochim. Acta 62 (12), 2039–2051.
Iff, N., Renforth, P., Pogge von Strandmann, P.A.E., 2024. The dissolution of olivine added to soil at 32°C: the fate of weathering products and its implications for enhanced weathering at different temperatures. Front. Clim. 6, 1252210.
Jacobson, A.D., Andrews, M.G., Lehn, G.O., Holmden, C., 2015. Silicate versus carbonate weathering in Iceland: new insights from Ca isotopes. Earth Planet Sci. Lett. 416, 132–142.
Jacobson, A.D., Blum, J.D., 2000. Ca/Sr and 87Sr/86Sr geochemistry of disseminated calcite in Himalayan silicate rocks from Nanga Parbat: influence on river-water chemistry. Geology 28, 463–466.
Jeffcoate, A.B., Elliott, T., Thomas, A., Bouman, C., 2004. Precise, small sample size determinations of lithium isotopic compositions of geological reference materials and modern seawater by MC-ICP-MS. Geostand. Geoanal. Res. 28 (1), 161–172.
Jones, M.T., Pearce, C.R., Oelkers, E.H., 2012. An experimental study of the interaction of basaltic riverine particulate material and seawater. Geochem. Cosmochim. Acta 77, 108–120.
Kennedy, M.J., Löhr, S.C., Fraser, S.A., Baruch, E.T., 2014. Direct evidence for organic carbon preservation as clay-organic nanocomposites in a Devonian black shale; from deposition to diagenesis. Earth Planet Sci. Lett. 388, 59–70.
Kennedy, M.J., Wagner, T., 2011. Clay mineral continental amplifier for marine carbon sequestration in a greenhouse ocean. In: Proceedings of the National Academy of Sciences, 108, pp. 9776–9781.
Kisakürek, B., James, R.H., Harris, N.B.W., 2005. Li and δ^7Li in Himalayan rivers: proxies for silicate weathering? Earth Planet Sci. Lett. 237 (3–4), 387–401.
Krause, A.J., Sluijs, A., van der Ploeg, R., Lenton, T.M., Pogge von Strandmann, P.A.E., 2023. Enhanced clay formation key in sustaining the middle eocene climatic optimum. Nat. Geosci. 16, 730–738.
Lalonde, K., Mucci, A., Ouellet, A., Gelinas, Y., 2012. Preservation of organic matter in sediments promoted by iron. Nature 483, 198–200.
Lasaga, A.C., Soler, J.M., Ganor, J., Burch, T.E., Nagy, K.L., 1994. Chemical weathering rate laws and global geochemical cycles. Geochem. Cosmochim. Acta 58 (10), 2361–2386.
Lemarchand, E., Chabaux, F., Vigier, N., Millot, R., Pierret, M.C., 2010. Lithium isotope systematics in a forested granitic catchment (Strengbach, Vosges Mountains, France). Geochem. Cosmochim. Acta 74, 4612–4628.
Li, W., Liu, X.-M., 2020. Experimental investigation of lithium isotope fractionation during kaolinite adsorption: implications for chemical weathering. Geochem. Cosmochim. Acta 284, 156–172.
Little, S.H., Munson, S., Prytulak, J., Coles, B.J., Hammond, S.J., Widdowson, M., 2019. Cu and Zn isotope fractionation during extreme chemical weathering. Geochem. Cosmochim. Acta 263, 85–107.
Liu, C.-Y., Pogge von Strandmann, P.A.E., Tarbuck, G., Wilson, D.J., 2022. Experimental investigation of oxide leaching methods for Li isotopes. Geostand. Geoanal. Res. 46 (3), 493–518.
Liu, X.-M., Wanner, C., Rudnick, R.L., McDonough, W.F., 2015. Processes controlling δ7Li in rivers illuminated by study of streams and groundwaters draining basalts. Earth Planet Sci. Lett. 409, 212–224.
Louvat, P., Allegre, C.J., 1997. Present denudation rates on the island of Reunion determined by river geochemistry: basalt weathering and mass budget between chemical and mechanical erosions. Geochem. Cosmochim. Acta 61 (17), 3645–3669.
Louvat, P., Gislason, S.R., Allegre, C.J., 2008. Chemical and mechanical erosion rates in Iceland as deduced from river dissolved and solid material. Am. J. Sci. 308, 679–726.
Maffre, P., Godderis, Y., Vigier, N., Moquet, J.-S., Carretier, S., 2020. Modelling the riverine δ7Li variability throughout the Amazon Basin. Chem. Geol., 119336
Millot, R., Scaillet, B., Sanjuan, B., 2010. Lithium isotopes in island arc geothermal systems: Guadeloupe, Martinique (French West Indies) and experimental approach. Geochem. Cosmochim. Acta 74 (6), 1852–1871.
Misra, S., Froelich, P.N., 2012. Lithium isotope history of cenozoic seawater: changes in silicate weathering and reverse weathering. Science 335, 818–823.
Murphy, M.J., Porcelli, D., Pogge von Strandmann, P.A.E., Hirst, C.A., Kutscher, L., Katchinoff, J.A., Mörth, C.-M., Maximov, T., Andersson, P.S., 2019. Tracing silicate weathering processes in the permafrost-dominated Lena River watershed using lithium isotopes. Geochem. Cosmochim. Acta 245, 154–171.
Oelkers, E.H., Butcher, R., Pogge von Strandmann, P.A.E., Schuessler, J.A., von Blanckenburg, F., Snaebjornsdottir, S.O., Mesfin, K., Aradottir, E.S.P., Gunnarsson, I., Sigfusson, B., Gunnlaugsson, E., Matter, J.M., Stute, M., Gislason, S. R., 2019. Using stable Mg isotope signatures to assess the fate of magnesium during the in situ mineralisation of CO2 and H2S at the CarbFix site in SW-Iceland. Geochem. Cosmochim. Acta 245, 542–555.
Parkhurst, D.L., Appelo, C.A.J., 1999. User's guide to PHREEQC (version 2) - a computer program for speciation, batch-reaction. One-Dimensional Transport, and Inverse Geochemical Calculations.
Pistiner, J.S., Henderson, G.M., 2003. Lithium-isotope fractionation during continental weathering processes. Earth Planet Sci. Lett. 214 (1–2), 327–339.
Pogge von Strandmann, P.A.E., Burton, K.W., James, R.H., van Calsteren, P., Gislason, S. R., 2010. Assessing the role of climate on uranium and lithium isotope behaviour in rivers draining a basaltic terrain. Chem. Geol. 270, 227–239.
Pogge von Strandmann, P.A.E., Burton, K.W., James, R.H., van Calsteren, P., Gislason, S. R., Mokadem, F., 2006. Riverine behaviour of uranium and lithium isotopes in an actively glaciated basaltic terrain. Earth Planet Sci. Lett. 251, 134–147.
Pogge von Strandmann, P.A.E., Burton, K.W., Opfergelt, S., Eiriksdottir, E.S., Murphy, M. J., Einarsson, A., Gislason, S.R., 2016. The effect of hydrothermal spring weathering processes and primary productivity on lithium isotopes: lake Myvatn, Iceland. Chem. Geol. 445, 4–13.
Pogge von Strandmann, P.A.E., Burton, K.W., Opfergelt, S., Genson, B., Guicharnaud, R. A., Gislason, S.R., 2021a. The lithium isotope response to the variable weathering of soils in Iceland. Geochem. Cosmochim. Acta 313, 55–73.
Pogge von Strandmann, P.A.E., Burton, K.W., Snaebjornsdottir, S.O., Sigfusson, B., Aradottir, E.S.P., Gunnarsson, I., Alfredsson, H.A., Mesfin, K.G., Oelkers, E.H., Gislason, S.R., 2019a. Rapid CO2 mineralisation into calcite at the CarbFix storage site quantified using calcium isotopes. Nat. Commun. 10, 1983. https://doi.org/10.1038/s41467-019-10003-8.
Pogge von Strandmann, P.A.E., Cosford, L.R., Liu, C.-Y., Liu, X., Krause, A.J., Wilson, D. J., He, X., McCoy-West, A.J., Gislason, S.R., Burton, K.W., 2023. Assessing hydrological controls on the lithium isotope weathering tracer. Chem. Geol. 642, 121801.
Pogge von Strandmann, P.A.E., Fraser, W.T., Hammond, S.J., Tarbuck, G., Wood, I.G., Oelkers, E.H., Murphy, M.J., 2019b. Experimental determination of Li isotope behaviour during basalt weathering. Chem. Geol. 517, 34–43.
Pogge von Strandmann, P.A.E., Frings, P.J., Murphy, M.J., 2017. Lithium isotope behaviour during weathering in the ganges alluvial plain. Geochem. Cosmochim. Acta 198, 17–31.
Pogge von Strandmann, P.A.E., Henderson, G.M., 2015. The Li isotope response to mountain uplift. Geology 43 (1), 67–70.
Pogge von Strandmann, P.A.E., James, R.H., van Calsteren, P., Gíslason, S.R., Burton, K. W., 2008. Lithium, magnesium and uranium isotope behaviour in the estuarine environment of basaltic islands. Earth Planet Sci. Lett. 274 (3–4), 462–471.
Pogge von Strandmann, P.A.E., Jones, M.T., West, A.J., Murphy, M.J., Stokke, E.W., Tarbuck, G., Wilson, D.J., Pearce, C.R., Schmidt, D.N., 2021b. Lithium isotope evidence for enhanced weathering and erosion during the Paleocene-Eocene Thermal Maximum. Sci. Adv. 7, eabh4224.
Pogge von Strandmann, P.A.E., Kasemann, S.A., Wimpenny, J.B., 2020. Lithium and lithium isotopes in earth's surface cycles. Elements 16, 253–258.
Pogge von Strandmann, P.A.E., Liu, X., Liu, C.Y., Wilson, D.J., Hammond, S.J., Tarbuck, G., Aristilde, L., Krause, A.J., Fraser, W.T., 2022a. Lithium isotope behaviour during basalt weathering experiments amended with organic acids. Geochem. Cosmochim. Acta 328, 37–57.
Pogge von Strandmann, P.A.E., Olsson, J., Luu, T.-H., Gislason, S.R., Burton, K.W., 2019c. Using Mg isotopes to estimate natural calcite compositions and precipitation rates during the 2010 Eyjafjallajökull eruption. Front. Earth Sci. 7.
Pogge von Strandmann, P.A.E., Renforth, P., West, A.J., Murphy, M.J., Luu, T.-H., Henderson, G.M., 2021c. The lithium and magnesium isotope signature of olivine dissolution in soil experiments. Chem. Geol. 560, 120008.
Pogge von Strandmann, P.A.E., Tooley, C., Mulders, J.J.P.A., Renforth, P., 2022b. The dissolution of olivine added to soil at 4°C: implications for enhanced weathering in cold regions. Front. Clim. 4, 827698.
Ramos, E.J., Breecker, D.O., Barnes, J.D., Li, F., Gingerich, P.D., Loewy, S.L., Satkoski, A. M., Baczynski, A.A., Wing, S.L., Miller, N.R., Lassiter, J.C., 2022. Swift weathering response on floodplains during the paleocene-eocene thermal maximum. Geophys. Res. Lett. 49 (6), e2021GL097436.
Renforth, P., 2012. The potential of enhanced weathering in the UK. Int. J. Greenh. Gas Control 10, 229–243.
Renforth, P., Pogge von Strandmann, P.A.E., Henderson, G.M., 2015. The dissolution of olivine added to soil: implications for enhanced weathering. Appl. Geochem. 61, 109–118.
Sauzéat, L., Rudnick, R.L., Chauvel, C., Garcon, M., Tang, M., 2015. New perspectives on the Li isotopic composition of the upper continental crust and its weathering signature. Earth Planet Sci. Lett. 428, 181–192.
Sproson, A.D., Pogge von Strandmann, P.A.E., Selby, D., Jarochowska, E., Fryda, J., Hladil, J., Loydell, D.K., Slavik, L., Calner, M., Maier, G., Munnecke, A., Lenton, T. M., 2022. Osmium and lithium isotope evidence for weathering feedbacks linked to orbitally paced organic carbon burial and Silurian glaciations. Earth Planet Sci. Lett. 577, 117260.
Stefansson, A., Gislason, S.R., 2001. Chemical weathering of basalts, Southwest Iceland: effect of rock crystallinity and secondary minerals on chemical fluxes to the ocean. Am. J. Sci. 301 (6), 513–556.
Steinhoefel, G., Brantley, S.L., Fantle, M.S., 2021. Lithium isotopic fractionation during weathering and erosion of shale. Geochem. Cosmochim. Acta 295, 155–177.
Tessier, A., Campbell, P.G.C., Bisson, M., 1979. Sequential extraction procedure for the speciation of particulate trace metals. Anal. Chem. 51 (7), 844–851.
Vigier, N., Decarreau, A., Millot, R., Carignan, J., Petit, S., France-Lanord, C., 2008. Quantifying Li isotope fractionation during smectite formation and implications for the Li cycle. Geochem. Cosmochim. Acta 72, 780–792.
Vigier, N., Gislason, S.R., Burton, K.W., Millot, R., Mokadem, F., 2009. The relationship between riverine lithium isotope composition and silicate weathering rates in Iceland. Earth Planet Sci. Lett. 287 (3–4), 434–441.
Walker, J.C.G., Hays, P.B., Kasting, J.F., 1981. A negative feedback mechanism for the long-term stabilization of earths surface-temperature. J. Geophy. Res. Oceans Atmos. 86 (NC10), 9776–9782.

West, A.J., Galy, A., Bickle, M., 2005. Tectonic and climatic controls on silicate weathering. Earth Planet Sci. Lett. 235 (1–2), 211–228.
Wilson, D.J., Pogge von Strandmann, P.A.E., White, J., Tarbuck, G., Marca, A.D., Atkinson, T.C., Hopley, P.J., 2021. Seasonal variability in silicate weathering signatures recorded by Li isotopes in cave drip-waters. Geochem. Cosmochim. Acta 312, 194–216.
Wimpenny, J., Colla, C.A., Yu, P., Yin, Q.Z., Rustad, J.R., Casey, W.H., 2015. Lithium isotope fractionation during uptake by gibbsite. Geochem. Cosmochim. Acta 168, 133–150.
Wimpenny, J., Gislason, S.R., James, R.H., Gannoun, A., Pogge von Strandmann, P.A.E., Burton, K.W., 2010. The behaviour of Li and Mg isotopes during primary phase dissolution and secondary mineral formation in basalt. Geochem. Cosmochim. Acta 74, 5259–5279.
Zhang, F., Dellinger, M., Hilton, R.G., Yu, J., Allen, M.B., Densmore, A.L., Sun, H., Jin, Z., 2022. Hydrological control of river and seawater lithium isotopes. Nat. Commun. 13, 3359.
Zhang, X.Y., Wilson, D.J., Hamers, M.F., Pogge von Strandmann, P.A.E., Mulders, J.J.P. A., Plümper, O., King, H.E., 2025. Coupling of Li–Fe: Li isotope fractionation during sorption onto Fe-oxides. ACS Earth Space Chem. 9 (1), 49–63.